HHS Public Access

Author manuscript

Biochim Biophys Acta. Author manuscript; available in PMC 2017 September 01.

Published in final edited form as:

Biochim Biophys Acta. 2016 September ; 1860(9): 1845–1853. doi:10.1016/j.bbagen.2016.05.029.

Enzyme-Specific Differences in Mannose Phosphorylation Between GlcNAc-1-Phosphotransferase αβ and γ subunit Deficient Zebrafish Support Cathepsin Proteases As Early Mediators of Mucolipidosis Pathology

Heather Flanagan-Steet, **Courtney Matheny**, **Aaron Petrey**, **Joshua Parker**, and **Richard Steet**

Complex Carbohydrate Research Center, 315 Riverbend Road, University of Georgia, Athens, GA 30602

Abstract

Targeting soluble acid hydrolases to lysosomes requires the addition of mannose 6-phosphate residues on their N-glycans. This process is initiated by GlcNAc-1-phosphotransferase, a multi-subunit enzyme encoded by the *GNPTAB* and *GNPTG* genes. The *GNPTAB* gene products (the α and β subunits) are responsible for recognition and catalysis of hydrolases whereas the *GNPTG* gene product (the γ subunit) enhances mannose phosphorylation of a subset of hydrolases. Here we identify and characterize a zebrafish *gnptg* insertional mutant and show that loss of the gamma subunit reduces mannose phosphorylation on a subset glycosidases but does not affect modification of several cathepsin proteases. We further show that glycosidases, but not cathepsins, are hypersecreted from *gnptg*$^{-/-}$ embryonic cells, as evidenced by reduced intracellular activity and increased circulating serum activity. The *gnptg*$^{-/-}$ embryos lack the gross morphological or craniofacial phenotypes shown in *gnptab*-deficient morphant embryos to result from altered cathepsin activity. Despite the lack of overt phenotypes, decreased fertilization and embryo survival were noted in mutants, suggesting that *gnptg* associated deposition of mannose 6-phosphate modified hydrolases into oocytes is important for early embryonic development. Collectively, these findings demonstrate that loss of the zebrafish GlcNAc-1-phosphotransferase γ subunit causes enzyme-specific effects on mannose phosphorylation. The finding that cathepsins are normally modified in *gnptg*$^{-/-}$ embryos is consistent with data from *gnptab*-deficient zebrafish suggesting these proteases are the key mediators of acute pathogenesis. This work also establishes a valuable new model that can be used to probe the functional relevance of *GNPTG* mutations in the context of a whole animal.

To whom correspondence should be addressed: Richard Steet, Ph.D. Associate Professor of Biochemistry and Molecular Biology, Complex Carbohydrate Research Center, University of Georgia, 315 Riverbend Road, Athens, GA 30602, Telephone: (706) 583-5550; Fax: (706) 542-4412; rsteet@ccrc.uga.edu.

Author Contributions

CM, AP, and JP performed experiments. HFS and RS conceived and performed experiments, interpreted data, and wrote the paper.

Graphical Abstract

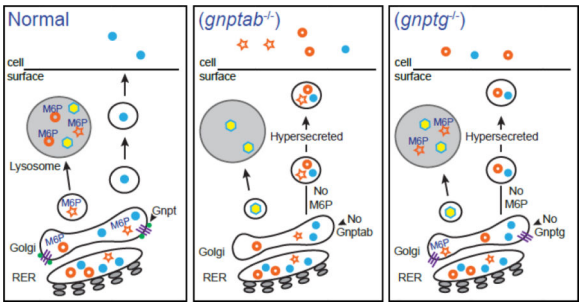

Keywords

lysosomal hydrolase; zebrafish; cathepsin; mannose phosphorylation

Introduction

The sorting of soluble acid hydrolases to lysosomes is a carbohydrate-dependent process that relies on receptor-mediated transport of enzymes whose N-linked glycans are modified with mannose 6-phosphate (M6P) residues (1). M6P residues are generated by a two-step process initiated in the Golgi by the UDP-GlcNAc:lysosomal enzyme GlcNAc-1-phosphotransferase. GlcNAc-1-phosphotransferase is an α2β2γ2 heterohexamer encoded by two genes. The *gnptab* gene encodes the α/β precursor that is proteolytic cleaved in the Golgi to generate the α and β subunits; the *gnptg* gene encodes the gamma (γ) subunit (2,3). The ability to specifically recognize acid hydrolases and to catalyze the transfer of GlcNAc-phosphate to the glycans is mediated by conserved domains within the α and β subunits (4–6). The functional relevance of the γ subunit is less defined. Prior work in *Gnptg*-deficient mice has shown that this subunit is required for efficient mannose phosphorylation of a subset of hydrolases, but a direct role in hydrolase binding has not been established (7,8).

Loss-of-function mutations in *GNPTAB* cause the multi-system diseases mucolipidosis II (MLII) and mucolipidosis IIIαβ (MLIIIαβ)(9,10). Mutations in *GNPTG* result in an attenuated form of ML disease (mucolipidosis IIIgamma; MLIIIgamma) and, like the other genes within this pathway, have also been associated with persistent stuttering (2,11–15). The γ subunit contains an MRH (mannose-6-phosphate receptor homology) domain similar to those found in ER glucosidase II (16). Since many MRH domains act as lectins that bind both M6P modified and non-modified high mannose oligosaccharides, its presence in the γ subunit suggests that it might facilitate subunit ability to bind the N-glycans of hydrolases, thereby modulating the αβ's recognition capability (17). It was also suggested that the MRH domain binds glycans on the α subunit, but a recent study demonstrated that interaction between the αβ and γ subunits is MRH-independent (18).

Analyses of *Gnptab* and *Gnptg* null mice have demonstrated differences in the phenotypic consequences associated with loss of the two genes (19,20). In particular, cellular lesions were not only less severe but also more restricted in *Gnptg*$^{-/-}$ mice. Additionally, unlike *Gnptab*$^{-/-}$ mice *Gnptg*$^{-/-}$ mice were normal in size and lacked cartilage defects. Despite

lacking intralysosomal storage, *gnptab*-deficient zebrafish also recapitulate many of the molecular phenotypes associated with MLII (21). Although both glycosidase and cathepsin protease mannose phosphorylation are impaired, the cartilage phenotypes in *gnptab*-deficient zebrafish embryos have been specifically linked to increased extracellular activity of certain cathepsin proteases (22,23). Furthermore, analysis of specific patient mutations in cells and in zebrafish suggests that the phenotypic variability noted in human patients may lie in the differential impact of these mutations on the mannose phosphorylation of specific lysosomal substrates (5,24,25). Catalytic transfer of GlcNAc-phosphate to hydrolase N-glycans first requires their recognition by GlcNAc-1-phosphotransferase. Therefore, mutations that alter its interaction with certain hydrolases may cause substrate-specific differences in M6P addition. As such, effects on specific hydrolases – not an overall reduction in phosphotransferase activity – may dictate the phenotypic variances associated with loss of *Gnptab* and *Gnptg*.

In order to further our understanding of the function of the γ subunit and assess disease specific mechanisms of reduced mannose phosphorylation, we identified and characterized a zebrafish line harboring a viral insertion that disrupts *gnptg* expression. Using this mutant line we uncovered new aspects of *gnptg* regulation and function during embryonic development. Consistent with a lack of gross phenotypes in *gnptg*$^{-/-}$ embryos, biochemical analyses revealed that glycosidase but not cathepsin mannose phosphorylation was impaired. These data indicate that the γ subunit promotes the mannose phosphorylation of a specific subset of lysosomal hydrolases. Despite the lack of MLII-like phenotypes, *gnptg*$^{-/-}$ embryos did exhibit decreased fertilization and embryo survival, suggesting *gnptg* may be important during early embryonic development. The implication of these and other findings on the regulation of GlcNAc-1-phosphotranserase activity during early development are discussed.

Results

Identification and characterization of *gnptg*-null zebrafish insertional mutant

Commercially generated *gnptg*^{TgZM00105646} mutant zebrafish containing a 4.6 kb viral insertion were obtained (Zenomics LLC) and transgenic founders identified by genomic PCR. Following genetic outcross, F3 transgenic carriers were mated and the progeny reared. Using a multiplex PCR strategy involving primer pairs targeting both viral (ISV, inside virus) and non-viral (OSV, outside virus) sequences, genotypes were assigned and homozygous transgenic animals identified (Figure 1A–B). RT-PCR analysis of *gnptg* gene expression in 3dpf (day post-fertilization) WT (+/+) progeny showed high levels of *gnptg* transcript, which was undetectable in progeny homozygous for the viral transgene (*gnptg*$^{Tg\ ZM00105646}$/*gnptg*$^{Tg\ ZM00105646}$; γ / γ; Figure 1C). Multiple amplicon regions positioned either 5’ or 3’ of the insertion were tested (see Materials and Methods). These data showed that viral insertion into exon 2 disrupted gene expression, generating a null allele, here forth referred to as *gnptg*$^{-/-}$. To further assess whether loss of the gamma (γ) subunit affected the GlcNAc-1-phosphotransferase enzyme, its activity towards a simple sugar substrate was tested and found comparable in *gnptg*$^{-/-}$ and control embryos (Figure 1D). This is in contrast to embryos deficient for the αβ subunit (*gnptab* morphants), which typically only exhibited 15–20% of WT activity. These data indicate that loss of the γ

subunit does not reduce phosphotransferase activity towards a simple sugar substrate. Further, RT-PCR analyses of *gnptg*$^{-/-}$ embryos showed normal levels of *gnptab* mRNA, suggesting that the γ subunit does not influence αβ expression in this system, in contrast to what has been noted in cells (26,27).

gnptg$^{-/-}$ embryos exhibit reduced mannose phosphorylation of a subset of acid hydrolases

To address whether loss of the γ subunit impacts the mannose phosphorylation of lysosomal hydrolases, WT, *gnptab* morphant, and *gnptg*$^{-/-}$ mutant embryo lysates were fractionated using a cation independent mannose phosphate receptor (CI-MPR) affinity column. This method provides an indirect measure of mannose phosphorylation by determining the amount of enzyme activity that bears M6P residues. The activities of several glycosidases and cathepsin proteases were determined in the bound (M6P-containing) and unbound fractions. In 4dpf *gnptg*$^{-/-}$ embryos, mannose phosphorylation was nearly undetectable on multiple glycosidases, including β-galactosidase (Glb), β-glucuronidase (Gusb), α-hexosaminidase (Hexa), α-mannosidase (Man2b1), and α-iduronidase (Idua) (Figure 1E **and** Table I). In contrast the level of mannose phosphorylation of three different cathepsin (Cts) proteases (Ctsk, Ctsl, Ctss) remained high in *gnptg*$^{-/-}$ embryos compared to their substantial reduction in *gnptab* morphants (Figure 1F **and** Table I). Ctsd, which is normally minimally M6P modified, was not significantly affected in either *gnptg*$^{-/-}$ or *gnptab* deficient animals. Surprisingly the M6P levels noted in *gnptg*$^{-/-}$ embryos were even lower than those described in *gnptab* morphants (Figure 1E, (21)). In the case of α-mannosidase, there was no difference in the mannose phosphorylation of this glycosidase between WT and *gnptab* morphants despite a complete absence of this modification in the gnptg-null embryos. This is likely due to differences in the pools of maternally derived M6P-modified enzymes (see Discussion).

Since the steady-state levels of mannose phosphorylation in WT embryos were already relatively low, it is possible that the levels noted in *gnptg*$^{-/-}$ embryos underestimate the effect of γ subunit on M6P biosynthesis. Previous studies in mammals showed that the M6P residue is removed more slowly in lysosomes of the brain, yielding significantly higher steady-state levels (28,29). Therefore, to more accurately assess how loss of the γ subunit impacts M6P biosynthesis, mannose phosphorylation levels were also determined in brains isolated from WT and *gnptg*$^{-/-}$ adult fish. Similar to that noted in embryos, 28% of the β-galactosidase from WT brains was M6P modified with only 1% of the enzyme in *gnptg*$^{-/-}$ brains modified (Figure 1G **and** Table I). In contrast, the M6P levels on the cathepsin proteases were indistinguishable between WT and *gnptg*$^{-/-}$ brains (Figure 1H **and** Table I). Interestingly, comparison of WT levels showed that the cysteine cathepsin proteases, including K, L, and S, were normally more highly modified than either the aspartyl protease Ctsd or the lysosomal glycosidases, suggesting a greater dependence on M6P-dependent sorting.

Lysosomal glycosidase (but not cathepsin proteases) are hypersecreted from embryonic and adult cells

As demonstrated in multiple *gnptab*-deficienct models, complete loss of M6P biosynthesis profoundly alters skeletal tissue. To assess whether *gnptg* deletion affects developing chondrocytes, *gnptg*$^{-/-}$ adults were crossed into the *fli1a*:EGFP transgenic line, which expresses EGFP in endothelial cells, certain hematopoetic cells, and neural crest-derived craniofacial chondrocytes. As shown in Figure 2A, the intracellular activity of multiple enzymes, including β-galactosidase, was drastically reduced within both GFP-positive (chondrocyte-enriched) and GFP-negative cells isolated from dissociated *gnptg*$^{-/-}$;*fli1a*:EGFP transgenic embryos. Because the activities of these enzymes were indistinguishable in lysates of whole WT and mutant animals (23), these data suggest that in *gnptg*$^{-/-}$ cells the majority of enzyme resides in the extracellular space. In contrast to the galactosidases, the activity of acid α-glucosidase, a lysosomal hydrolase that is not M6P modified in zebrafish (30), was similar within WT and mutant cells (Figure 2B). Additionally, the intracellular levels of two highly modified cathepsins (Ctsk and Ctsl), and the minimally modified Ctsd, were all also indistinguishable between WT and *gnptg*$^{-/-}$ sorted cells (Figure 2C–E). The lack of cathepsin hypersecretion is further supported by confocal analyses of Ctsk localization. We previously demonstrated Ctsk's presence in the extracellular space outside chondrocytes lacking the αβ subunit (22). Analyses of GFP-labeled *gnptg*$^{-/-}$ chondrocytes, however, showed only intracellular Ctsk (Figure 2F). This is evidenced by complete overlap between cellular GFP (green) and immunohistochemically stained Ctsk (red). Ctsk staining was never detected outside WT or *gnptg*$^{-/-}$ cells.

Despite the attenuated clinical presentation of MLIIIαβ, patients with mutations in the *GNPTG* gene have significantly elevated levels of serum glycosidases (2). To ask whether glycosidases also accumulate in the bloodstream of zebrafish, blood serum was isolated from WT and *gnptg*$^{-/-}$ adults and the activities of β-glucuronidase and β-hexosaminidase measured. Both activities were normalized to acid α-glucosidase, which was previously shown in zebrafish to lack the M6P modification (30). The absolute activity level of acid α-glucosidase was similar in serum isolated from *gnptg*$^{-/-}$ and WT adults. In contrast, β-galactosidase and β-hexosaminidase activities (relative to α-glucosidase) were elevated (~5-fold) in *gnptg*$^{-/-}$ serum, indicating that these glycosidases are secreted and stably accumulate in the bloodstream of mutant animals. The activity of any circulating cathepsin proteases was too low to measure in either WT or *gnptg*$^{-/-}$ animals.

gnptg$^{-/-}$ embryos do not exhibit any gross developmental defects

Microscopic analyses of *gnptg*$^{-/-}$ embryos revealed no overt morphological or behavioral defects (Figure 3A). In contrast to *gnptab* morphants, Alcian blue stained *gnptg*$^{-/-}$ cartilage was indistinguishable from age matched controls (Figure 3B)(21,23). In addition, confocal analyses of craniofacial structures in *gnptg*$^{-/-}$;*fli1a*:EGFP embryos, where chondrocytes are labeled with EGFP, also showed normal chondrocyte morphology and normal expression of the chondrogenic marker, type II collagen (Figure 3C). This is unlike loss of the β subunit, which not only alters chondrocyte organization but also drastically increases expression of type II collagen (21,23). Lastly, histologically stained sections of adult *gnptg*$^{-/-}$ animals were unremarkable compared to WT control sections. These data are consistent with the

finding that several cathepsin proteases, including Ctsk and Ctsl, are normally M6P modified in *gnptg*$^{-/-}$ embryos.

Despite a lack of obvious phenotypes in surviving *gnptg*$^{-/-}$ animals, progeny of *gnptg*$^{-/-}$ females exhibited reduced survival during the first 24hpf. Microscopic analyses of newly layed eggs showed that 31% of *gnptg*$^{-/-}$ embryos remain single-celled never undergoing cleavage (Figure 3D, E). This phenotype is noted in <10% of either homozygous WT embryos or heterozygous progeny of WT mothers and *gnptg*$^{-/-}$ fathers. Importantly, 37% of the heterozygous progeny of *gnptg*$^{-/-}$ females and WT males also remained unicellular, suggesting that this phenotype, which could stem either from reduced fertilization or aberrant cleavage, is due to maternal effects from loss of the γ subunit (Figure 3E). Although noted differences in survival wane significantly by 24 hpf, heterozygous progeny of either *gnptg*$^{-/-}$ mothers or fathers continue to exhibit slightly reduced survival rates up to 5 dpf. In addition, *gnptg*$^{-/-}$ embryos develop more slowly than WT embryos. This is evident during both cleavage and gastrulation (Figure 3E and F, respectively), with mutant embryos reaching defined developmental stages several hours after WT controls. Typically by 2–2.5 hpf ~85% of WT embryos contain 125–256 cells. At 2.5 hpf the majority of γ embryos are still 8–16 cell stage (Figure 3E). Slower growth was also evident 6 hpf (shield stage) where WT embryonic tissue (outlined in yellow) extends to the egg midline (white line), but *gnptg*$^{-/-}$ embryos are only partially extended.

gnptg$^{-/-}$ embryos exhibit differences in the modification of hydrolases maternally deposited within eggs

To address the possibility that differences in maternally deposited enzymes were associated with reduced survival and slower development of *gnptg*$^{-/-}$ embryos, we assessed the M6P levels in 0 to 3dpf embryos derived from four unique genetic crosses. These included: WT ♀ × WT ♂ (Cross 1), *gnptg*$^{-/-}$ ♀ × *gnptg*$^{-/-}$ ♂ (Cross 2), WT ♀ × *gnptg*$^{-/-}$ ♂ (Cross 3), and *gnptg*$^{-/-}$ ♀ × WT ♂ (Cross 4) (Figure 4A **and** Figure 5 Table II – III). For these analyses embryonic lysates were fractionated over a CI-MPR affinity column and the α- and β-galactosidase activities determined in the bound (M6P modified) and unbound fractions. At 0 dpf, 50–80% of these glycoidases were M6P modified in progeny of WT mothers (Crosses 1 and 3). In contrast both homozygous null and heterozygous progeny of *gnptg*$^{-/-}$ mothers (Crosses 2 and 4) exhibited a significant reduction in enzyme modification, with only 2–4% of the total enzyme present in the bound fraction (Figure 4B **and** Figure 5 Table II). Despite a drastic reduction in the M6P levels, total enzyme activity was unchanged. By 3 dpf, M6P levels in progeny of WT mothers (Crosses 1 and 3) also drop substantially with only 5 and 11% of the activity present in the bound fraction (Figure 4B **and** Figure 5 Table III); the level of M6P-modification on these enzymes again increased as the embryos developed (**see** Table I **and** Figure 5 Table IV). Because all residual yolk was removed prior to fractionation, the substantial decrease in 3dpf WT M6P levels could either reflect low-level modification of newly synthesized embryonic enzyme or residual maternally modified glycosidase that was actively transported from the yolk into the embryo. However, the fact that from 0–3dpf β-galactosidase in creases from 2% modified to 11% modified in heterozygous progeny of *gnptg*$^{-/-}$ mothers (Cross 4), but not *gnptg*$^{-/-}$ progeny from cross 2, suggests this is primarily due to modification of newly synthesized enzyme.

To further ask whether maternally deposited or embryonically expressed GlcNAc-1-phosphotransferase enzyme complexes primarily contribute to M6P modification of newly synthesized glycosidases, embryonic expression of *gnptab* was inhibited in the progeny of crosses 1, 3, and 4. Reducing *gnptab* expression in either homozygous WT eggs (Cross 1) or heterozygous eggs from *gnptg*$^{-/-}$ fathers (Cross 3) did not significantly alter the levels of M6P-modified α or β-galactosidase present 3dpf (Figure 4C). However, reduced levels of M6P-modification were detectable in *gnptab*-inhibited embryos at 4dpf, perhaps reflecting the disappearance of maternally deposited GlcNAc-1-phosphotransferase complexes (Table I, (21)). A role for maternally deposited enzyme complexes is further supported by the fact that the levels of M6P-modified α and β-galactosidase rise more slowly in heterozygous progeny of *gnptg*$^{-/-}$ mothers (Cross 4) than the heterozygous progeny of *gnptg*$^{-/-}$ fathers (Cross 3) (Figure 5 Table IV). Embryos from both crosses express the γ subunit, but those with *gnptg*$^{-/-}$ mothers do not have γ subunit deposited into the egg. Clearly embryonic synthesis of GlcNAc-1-phosphotransferase complexes can also contribute to rising M6P levels during the first several days of development. This is illustrated by the fact that *gnptab*-inhibition in heterozygous progeny of *gnptg*$^{-/-}$ mothers (Cross 4) reduces M6P-modified glycosidase to those that are indistinguishable from αβ-positive *gnptg*$^{-/-}$ progeny.

Discussion

The present findings demonstrate selective effects on the mannose phosphorylation of lysosomal hydrolases in zebrafish lacking the γ subunit of the Glc-NAc-1-phosphotransferase enzyme complex (*gnptg*$^{-/-}$). This observation mirrors results in *Gnptg*-null mice where the γ subunit was shown to be necessary for M6P-modification of certain hydrolases but dispensable for others. Importantly, our analyses in zebrafish extend the mouse studies by demonstrating that the modification of several cathepsin proteases is unaffected in *gnptg*$^{-/-}$ embryos. This is consistent with their lack of overt phenotypes, which were previously linked in *gnptab*-deficient animals to reduced mannose phosphorylation of Ctsk. Loss of M6P on Ctsk was associated with its increased extracellular activity and phenotypic onset (22,23). The fact that both parameters are unaltered in *gnptg*$^{-/-}$ animals further supports the idea that cathepsin proteases play a central and specific role in MLII disease pathology.

The basis for the selective effects of γ subunit on glycosidase mannose phosphorylation in the zebrafish system is unclear. Studies in brains from *Gnptg* adult mice did not reveal an obvious requirement for the γ subunit in the mannose phosphorylation of one hydrolase type versus another (8). It is possible that the robust effects of γ subunit depletion on glycosidase modification in zebrafish arise from the high level of expression in the proliferating cells of the embryo – and thus the need for highly efficient mannose phosphorylation in some tissues. The prior observation that loss of the γ subunit affected the rate of mannose phosphorylation (i.e. V_{max}) but not the binding (i.e. K_M) of hydrolases would support a role for this subunit in maintaining maximal catalytic function during certain stages of development (8). We cannot rule out the possibility that because cathepsins may also be sorted to different compartments in the embryo (such as secretory lysosomes) they may experience less dynamic removal of the M6P tag or protein turnover.

Although surviving *gnptg*$^{-/-}$ animals do not exhibit obvious phenotypes, reduced survival and slower rates of development were noted in both homozygous *gnptg*$^{-/-}$ embryos and heterozygous progeny of *gnptg*$^{-/-}$ mothers. These phenotypes were associated with reduced levels of M6P-modification on several maternally deposited glycosidases, including α and β-galactosidase. Loss of M6P-modification on these glycosidases correlated with a dramatic increase in the number of embryos remaining single-celled. It is currently unclear whether the increase in single-celled eggs primarily results from reduced fertilization or disrupted cleavage. However, studies in reproductive biology support a role for secreted glycosidases during fertilization. Reports from several groups suggest that extracellular glycosidase activity alters the carbohydrate composition of the zona pellucida preventing polyspermy (31–34). Because the activity levels of glycosidase were similar in WT and *gnptg*$^{-/-}$ embryos, our data support the possibility that M6P-based targeting mechanisms may be important for regulated release of glycosidase enzymes during such fertilization events. Since *gnptg*$^{-/-}$ embryos also develop substantially more slowly than WT embryos, it is also likely that M6P-mediated delivery of maternally deposited glycosidases to the developing embryo is equally important (albeit not essential) for early embryonic development.

One notable consideration in this study is the fact that different methods were used to create *gnptg*-null and *gnptab*-deficient embryos. In the case of the *gnptg*-null line, we had the advantage of maintaining this line as homozygotes due to the lack of major phenotypes. By doing so, we were able to track the influence of the γ subunit on maternal deposition of M6P-bearing hydrolases; this is evidenced by the complete lack of mannose phosphorylation on glycosidases in eggs derived from *gnptg*-null females. For *gnptab*-knockdown embryos, the mannose phosphorylation of maternally deposited enzymes is unaffected since WT eggs are used for morpholino knockdown of either maternal or embryonic transcripts. Since morpholinos won't impact phosphotransferase enzyme that is already made, any enzyme that was maternally deposited into eggs will remain active. This deposition into the yolk likely explains why the level of mannose phosphorylation on α-mannosidase – by far the most abundant glycosidase in zebrafish eggs - was unaffected in *gnptab* morphants (30).

A number of point mutations have now been identified within the *GNPTG* gene in humans, associated with both MLIIIγ and persistent stuttering. Those mutations that cause MLIIIγ lie in regions of the protein for which a clear function has yet to be assigned. The development and characterization of this zebrafish model will allow the impact of these mutations to be assessed in a whole organism via rescue experiments, further extending our understanding of this subunit.

Methods

Zebrafish strains and husbandry

Animals were maintained according to standard protocols. WT and transgenic zebrafish strains were obtained from the Zebrafish International Resource Center (ZIRC, Eugene, OR): Tg(*fli1a*:EGFP)^{y1}(35). The *gnptg* insertional mutant (ZeneMarker ID ZM00105646) was obtained from Zenomics LLC (Oregon; *this company no longer exists*). Staging was according to established criteria (36). In some cases 0.003% 1-phenyl 2-thiourea (PTU) was added to embryo medium to block pigmentation. Handling and euthanasia of fish for all

experiments complied with the University of Georgia policies, as approved by the UGA Institutional Animal Care and Use Committee (permit #A2013-8-144).

Genomic identification of gnptg$^{-/-}$ animals and reverse transcriptase-PCR analyses of gnptg expression

Zenomics provided identified F2 heterozygous adult carriers and F3 progeny of F2 heterozygotes crossed with WT animals. A multiplex PCR strategy involving a primer pair within the virus (ISV :For TAGGAGCTGTTGGAAAGCTTACCC and Rev AGTCTCCAGAAAAAGGGGGGAATG) and one outside the virus (OSV :For GATGGGCTGACTTTAGCCTG and Rev GACGTCATGAAACATGGCTG) was used to genotype fin-clipped adult animals. For RT-PCR analyses of transcript abundance, multiple primer pairs throughout the coding region were tested. These included primers targeting sequence upstream of the virus in exon 1 (For GGTGATGTTTTCAGTTGTCACATG and RevGCTGTCAGATAAAACAGGCATACTT), after the virus in exons 2 and 3 (For GCATACAGCGGTATACTGGT and RevGTCCAAAGCTTAAAACCCGT, and for the entire gene (For CAGTTGTCACATGAACACAGACG and Rev GTCCTGCATGGCTGAATAAAGT).

Morpholinos and inhibition of gene expression

Morpholino knockdown of GlcNAc-1-phosphotransferase was performed and assessed as previously described (21,23).

Histochemistry and Immunohistochemistry

Alcian blue staining was performed as previously described(21). Immunohistochemical analyses of type II collagen expression was performed as previously described (23). Bright field images were acquired on an Olympus SZ16 microscope with a Retiga 2000R camera and Q-capture software. Confocal images were acquired on an FV1000 laser scanning confocal microscope outfitted with a 60x (N.A.1.2) water immersion (whole mount images) or 60x (N.A.1.4) oil immersion lens (sections). Image projections and 3D reconstruction/ rotations were generated with Image J or Slidebook 5.0 (3i, Denver, CO) software. Final images were processed in Adobe Photoshop Extended.

FACS analyses of GFP (+) and (−) cells

fli1a:EGFP embryos were dissociated into single cell suspensions as previously described (23). GFP+ cells were sorted and counted as previously described (23). Enzyme assays were performed as previously described (30).

Enzyme activity assays and mannose 6-phosphate receptor affinity chromatography

Activity of lysosomal glycosidases was measured using the following fluorescent substrates: 4-methylumbelliferyl (MU) β-galactopyranoside (for β-galactosidase), 4-MU α-galactopyranoside (for α-galactosidase), 4-MU β-glucuronide (for β-glucuronidase), 4-MU β-Nacetylglucosaminide (for β-hexosaminidase), 4-MU α-iduropyranoside (for α-iduronidase) and 4-MU α-mannopyranoside (for acid α-mannosidase). All substrates were prepared in 50 mM sodium citrate or 100 mM sodium acetate reaction buffers, pH 4.5 with

0.5% Triton X-100 to a final concentration of 3 mM except for 4-MU α-iduropyranoside, which was prepared in formate buffer, pH 3.5 to a final concentration of 0.5 mM. Reactions were incubated for 16 h at 37°C, quenched with 0.2 M sodium carbonate buffer and the fluorescence of 4-methylumbelliferone was measured using a Turner 380 fluorometer. Lysates were fractionated using either a M6P receptor affinity column as previously described (21). The percentage of bound activity relative to total activity recovered from three independent experiments is shown.

Analysis of serum glycosidase activity

Adult zebrafish were anesthetized according to standard procedures using MS-222 and blood removed from the animal following scission of its tail fin. Blood was collected in tubes coated with heparin to prevent clotting. The blood was centrifuged (100 × g) for 5 mins at 4°C to remove cells. Glycosidase activity was measured in serum and the activity of acid α -glucosidase, an enzyme previously shown to not be mannose phosphorylated in zebrafish, was used to normalize the relative level of other glycosidases. This approach was used to overcome variations in the amount of serum obtained from different animals. The values shown represent the average of 5 independent serum samples isolated from either *gnptg*$^{-/-}$ adults or age-matched WT controls.

Statistical analyses

The two-tailed student *t*-test was used to compare statistical relevance of all experiments in which differences between two independent groups were compared. Student *t*-tests were run using Excel software version 14.5.5.

Acknowledgments

We would like to thank Dr. Peter Lobel (Rutgers University, NJ) for his generous contribution of the CI-MPR affinity matrix. We would also like to acknowledge Samantha Wright Leigh for technical assistance during this study. This work was supported by an NIH R01 (GM086524).

References

1. Kornfeld S, Mellman I. The biogenesis of lysosomes. Annual Review of Cell Biology. 1989; 5:483–525.
2. Raas-Rothschild, A.; Spiegel, R. Mucolipidosis III Gamma. In: Pagon, RA.; Adam, MP.; Ardinger, HH.; Wallace, SE.; Amemiya, A.; Bean, LJH.; Bird, TD.; Fong, CT.; Mefford, HC.; Smith, RJH.; Stephens, K., editors. GeneReviews(R). Seattle (WA): 1993.
3. Kudo M, Bao M, D'Souza A, Ying F, Pan H, Roe BA, Canfield WM. The alpha- and beta-subunits of the human UDP-N-acetylglucosamine:lysosomal enzyme N-acetylglucosamine-1-phosphotransferase [corrected] are encoded by a single cDNA. The Journal of Biological Chemistry. 2005; 280:36141–36149. [PubMed: 16120602]
4. Qian Y, Flanagan-Steet H, van Meel E, Steet R, Kornfeld SA. The DMAP interaction domain of UDP-GlcNAc:lysosomal enzyme N-acetylglucosamine-1-phosphotransferase is a substrate recognition module. Proceedings of the National Academy of Sciences of the United States of America. 2013; 110:10246–10251. [PubMed: 23733939]
5. Qian Y, van Meel E, Flanagan-Steet H, Yox A, Steet R, Kornfeld S. Analysis of mucolipidosis II/III GNPTAB missense mutations identifies domains of UDP-GlcNAc:lysosomal enzyme GlcNAc-1-phosphotransferase involved in catalytic function and lysosomal enzyme recognition. The Journal of Biological Chemistry. 2015; 290:3045–3056. [PubMed: 25505245]

6. Reitman ML, Kornfeld S. Lysosomal enzyme targeting. N-Acetylglucosaminylphosphotransferase selectively phosphorylates native lysosomal enzymes. The Journal of Biological Chemistry. 1981; 256:11977–11980. [PubMed: 6457829]
7. Lee WS, Payne BJ, Gelfman CM, Vogel P, Kornfeld S. Murine UDP-GlcNAc:lysosomal enzyme N-acetylglucosamine-1-phosphotransferase lacking the gamma-subunit retains substantial activity toward acid hydrolases. The Journal of Biological Chemistry. 2007; 282:27198–27203. [PubMed: 17652091]
8. Qian Y, Lee I, Lee WS, Qian M, Kudo M, Canfield WM, Lobel P, Kornfeld S. Functions of the alpha, beta, and gamma subunits of UDPGlcNAc: lysosomal enzyme N-acetylglucosamine-1-phosphotransferase. The Journal of Biological Chemistry. 2010; 285:3360–3370. [PubMed: 19955174]
9. Kudo M, Brem MS, Canfield WM. Mucolipidosis II (I-cell disease) and mucolipidosis IIIA (classical pseudo-hurler polydystrophy) are caused by mutations in the GlcNAc-phosphotransferase alpha / beta -subunits precursor gene. American Journal of Human Genetics. 2006; 78:451–463. [PubMed: 16465621]
10. Tiede S, Storch S, Lubke T, Henrissat B, Bargal R, Raas-Rothschild A, Braulke T. Mucolipidosis II is caused by mutations in GNPTA encoding the alpha/beta GlcNAc-1-phosphotransferase. Nature Medicine. 2005; 11:1109–1112.
11. Encarnacao M, Lacerda L, Costa R, Prata MJ, Coutinho MF, Ribeiro H, Lopes L, Pineda M, Ignatius J, Galvez H, Mustonen A, Vieira P, Lima MR, Alves S. Molecular analysis of the GNPTAB and GNPTG genes in 13 patients with mucolipidosis type II or type III - identification of eight novel mutations. Clinical Genetics. 2009; 76:76–84. [PubMed: 19659762]
12. Kang C, Riazuddin S, Mundorff J, Krasnewich D, Friedman P, Mullikin JC, Drayna D. Mutations in the lysosomal enzyme-targeting pathway and persistent stuttering. The New England Journal of Medicine. 2010; 362:677–685. [PubMed: 20147709]
13. Liu S, Zhang W, Shi H, Meng Y, Qiu Z. Three novel homozygous mutations in the GNPTG gene that cause mucolipidosis type III gamma. Gene. 2014; 535:294–298. [PubMed: 24316125]
14. Persichetti E, Chuzhanova NA, Dardis A, Tappino B, Pohl S, Thomas NS, Rosano C, Balducci C, Paciotti S, Dominissini S, Montalvo AL, Sibilio M, Parini R, Rigoldi M, Di Rocco M, Parenti G, Orlacchio A, Bembi B, Cooper DN, Filocamo M, Beccari T. Identification and molecular characterization of six novel mutations in the UDP-N-acetylglucosamine-1-phosphotransferase gamma subunit (GNPTG) gene in patients with mucolipidosis III gamma. Human Mutation. 2009; 30:978–984. [PubMed: 19370764]
15. Raza MH, Domingues CE, Webster R, Sainz E, Paris E, Rahn R, Gutierrez J, Chow HM, Mundorff J, Kang CS, Riaz N, Basra MA, Khan S, Riazuddin S, Moretti-Ferreira D, Braun A, Drayna D. Mucolipidosis types II and III and non-syndromic stuttering are associated with different variants in the same genes. European Journal of Human Genetics. 2016; 24:529–534. [PubMed: 26130485]
16. Olson LJ, Orsi R, Alculumbre SG, Peterson FC, Stigliano ID, Parodi AJ, D'Alessio C, Dahms NM. Structure of the lectin mannose 6-phosphate receptor homology (MRH) domain of glucosidase II, an enzyme that regulates glycoprotein folding quality control in the endoplasmic reticulum. The Journal of Biological Chemistry. 2013; 288:16460–16475. [PubMed: 23609449]
17. D'Alessio C, Dahms NM. Glucosidase II and MRH-domain containing proteins in the secretory pathway. Current Protein & Peptide Science. 2015; 16:31–48. [PubMed: 25692846]
18. van Meel E, Lee WS, Liu L, Qian Y, Doray B, Kornfeld S. Multiple Domains of GlcNAc-1-phosphotransferase Mediate Recognition of Lysosomal Enzymes. The Journal of Biological Chemistry. 2016; 291:8295–8307. [PubMed: 26833567]
19. Idol RA, Wozniak DF, Fujiwara H, Yuede CM, Ory DS, Kornfeld S, Vogel P. Neurologic abnormalities in mouse models of the lysosomal storage disorders mucolipidosis II and mucolipidosis III gamma. PloS One. 2014; 9:e109768. [PubMed: 25314316]
20. Vogel P, Payne BJ, Read R, Lee WS, Gelfman CM, Kornfeld S. Comparative pathology of murine mucolipidosis types II and IIIC. Veterinary Pathology. 2009; 46:313–324. [PubMed: 19261645]
21. Flanagan-Steet H, Sias C, Steet R. Altered chondrocyte differentiation and extracellular matrix homeostasis in a zebrafish model for mucolipidosis II. The American Journal of Pathology. 2009; 175:2063–2075. [PubMed: 19834066]

22. Flanagan-Steet H, Aarnio M, Kwan B, Guihard P, Petrey A, Haskins M, Blanchard F, Steet R. Cathepsin-Mediated Alterations in TGFss-Related Signaling Underlie Disrupted Cartilage and Bone Maturation Associated With Impaired Lysosomal Targeting. Journal of Bone and Mineral Research. 2016; 31:535–548. [PubMed: 26404503]

23. Petrey AC, Flanagan-Steet H, Johnson S, Fan X, De la Rosa M, Haskins ME, Nairn AV, Moremen KW, Steet R. Excessive activity of cathepsin K is associated with cartilage defects in a zebrafish model of mucolipidosis II. Disease models & mechanisms. 2016; 5:177–190. [PubMed: 22046029]

24. Leroy JG, Sillence D, Wood T, Barnes J, Lebel RR, Friez MJ, Stevenson RE, Steet R, Cathey SS. A novel intermediate mucolipidosis II/IIIalphabeta caused by GNPTAB mutation in the cytosolic N-terminal domain. European Journal of Human Genetics. 2014; 22:594–601. [PubMed: 24045841]

25. Zarghooni M, Dittakavi SS. Molecular analysis of cell lines from patients with mucolipidosis II and mucolipidosis III. American Journal of Medical Genetics. Part A. 2009; 149A:2753–2761. [PubMed: 19938078]

26. Pohl S, Tiede S, Marschner K, Encarnacao M, Castrichini M, Kollmann K, Muschol N, Ullrich K, Muller-Loennies S, Braulke T. Proteolytic processing of the gamma-subunit is associated with the failure to form GlcNAc-1-phosphotransferase complexes and mannose 6-phosphate residues on lysosomal enzymes in human macrophages. The Journal of Biological Chemistry. 2010; 285:23936–23944. [PubMed: 20489197]

27. Pohl S, Tiede S, Castrichini M, Cantz M, Gieselmann V, Braulke T. Compensatory expression of human N-acetylglucosaminyl-1-phosphotransferase subunits in mucolipidosis type III gamma. Biochimica et Biophysica Acta. 2009; 1792:221–225. [PubMed: 19708128]

28. Jadot M, Lin L, Sleat DE, Sohar I, Hsu MS, Pintar J, Dubois F, Wattiaux-De Coninck S, Wattiaux R, Lobel P. Subcellular localization of mannose 6- phosphate glycoproteins in rat brain. The Journal of Biological Chemistry. 1999; 274:21104–21113. [PubMed: 10409663]

29. Sleat DE, Sohar I, Lackland H, Majercak J, Lobel P. Rat brain contains high levels of mannose-6-phosphorylated glycoproteins including lysosomal enzymes and palmitoyl-protein thioesterase, an enzyme implicated in infantile neuronal lipofuscinosis. The Journal of Biological Chemistry. 1996; 271:19191–19198. [PubMed: 8702598]

30. Fan X, Klein M, Flanagan-Steet HR, Steet R. Selective yolk deposition and mannose phosphorylation of lysosomal glycosidases in zebrafish. The Journal of Biological Chemistry. 2010; 285:32946–32953. [PubMed: 20729204]

31. Cornwall GA, Tulsiani DR, Orgebin-Crist MC. Inhibition of the mouse sperm surface alpha-D-mannosidase inhibits sperm-egg binding in vitro. Biology of Reproduction. 1991; 44:913–921. [PubMed: 1868148]

32. Honegger TG, Koyanagi R. The ascidian egg envelope in fertilization: structural and molecular features. The International journal of Developmental Biology. 2008; 52:527–533. [PubMed: 18649266]

33. Takada M, Yonezawa N, Yoshizawa M, Noguchi S, Hatanaka Y, Nagai T, Kikuchi K, Aoki H, Nakano M. pH-sensitive dissociation and association of beta-N-acetylhexosaminidase from boar sperm acrosome. Biology of Reproduction. 1994; 50:860–868. [PubMed: 8199267]

34. Yonezawa N, Amari S, Takahashi K, Ikeda K, Imai FL, Kanai S, Kikuchi K, Nakano M. Participation of the nonreducing terminal beta-galactosyl residues of the neutral N-linked carbohydrate chains of porcine zona pellucida glycoproteins in sperm-egg binding. Molecular Reproduction and Development. 2005; 70:222–227. [PubMed: 15570618]

35. Lawson ND, Weinstein BM. In vivo imaging of embryonic vascular development using transgenic zebrafish. Developmental Biology. 2002; 248:307–318. [PubMed: 12167406]

36. Kimmel CB, Ballard WW, Kimmel SR, Ullmann B, Schilling TF. Stages of embryonic development of the zebrafish. Developmental Dynamics. 1995; 203:253–310. [PubMed: 8589427]

Highlights

- *gnptg*$^{-/-}$ zebrafish exhibit selective effects on hydrolase mannose phosphorylation
- glycosidases, but not cathepsins, are hypersecreted from *gnptg*$^{-/-}$ embryonic cells, as evidenced by reduced intracellular activity and increased circulating serum activity
- *gnptg*$^{-/-}$ embryos lack the gross morphological or craniofacial phenotypes shown in *gnptab*-deficient morphant embryos to result from altered cathepsin activity
- loss of gnptg expression in zebrafish results in decreased fertilization and embryo survival, suggesting that *gnptg* associated deposition of mannose 6-phosphate modified hydrolases into oocytes is important for early embryonic development

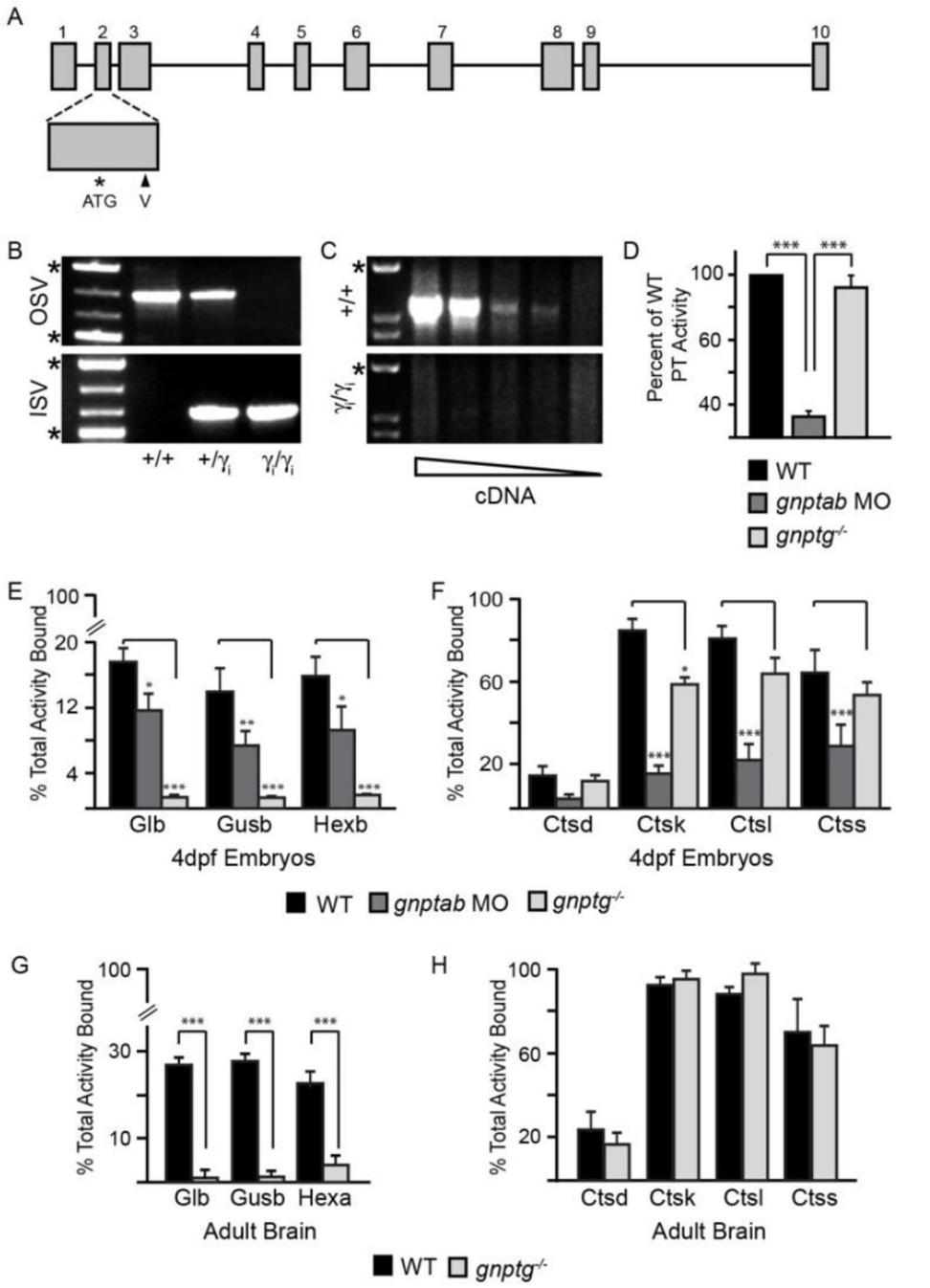

Figure 1. Loss of the GlcNAc-1-phosphotransferase γ subunit specifically reduces M6P addition to glycosidases without affecting modification of the cathepsin proteases

(A). Schematic shows insertion of a 4.6 kb virus into the second exon of *gnptg (γ)*. (B) Multi-plex PCR of genomic DNA isolated from adult zebrafish using primers targeting viral (inside virus, ISV) and non-viral (outside virus, OSV) sequences identified animals of various genotypes: homozygous WT (+/+), heterozygous (+/γ_i) and homozygous *gnptg*$^{-/-}$ (γ_i/γ_i). * marker bands indicate 1500 and 500bp, respectively. (C) RT-PCR of RNA isolated from 3dpf WT and *gnptg*$^{-/-}$ (γ_i/γ_i) embryos demonstrate complete loss of *gnptg* message in mutant animals. Analyses were performed over a gradient of cDNA concentrations. n=4

experiments of 20 embryos/condition. Each experiment represents a unique parental cross (i.e. biological replicate). * marker bands is 1500 bp. (D) Enzymatic analysis of phosphotransferase activity demonstrated similar activities in WT and *gnptg*$^{-/-}$ embryos that were significantly reduced in *gnptab*-deficient embryos. n=3 exper. with 60 embryos per lysate. (E-F) The percent of total glycosidase (E) or cathepsin (F) enzyme (activity) that is mannose phosphorylated in WT, *gnptab*-deficient morphants (MO), and *gnptg*$^{-/-}$ embryos 4dpf. n=100-150 embryos/condition over 4–7 experiments. Each experiment represents a unique parental cross (i.e. biological replicate). (G-H) The percent of total glycosidase (G) or cathepsin (H) enzyme (activity) that is mannose phosphorylated in the brains of WT and *gnptg*$^{-/-}$ adult zebrafish. n=10 brains/condition. * is $p<0.05$; ** is $p<0.01$; *** is $p<0.001$. β-galactosidase (Glb), β-glucuronidase (Gusb), β-hexosaminidase (Hexb). Cathepsin D (Ctsd), Cathepsin K (Ctsk), Cathepsin L (Ctsl), Cathepsin S (Ctss).

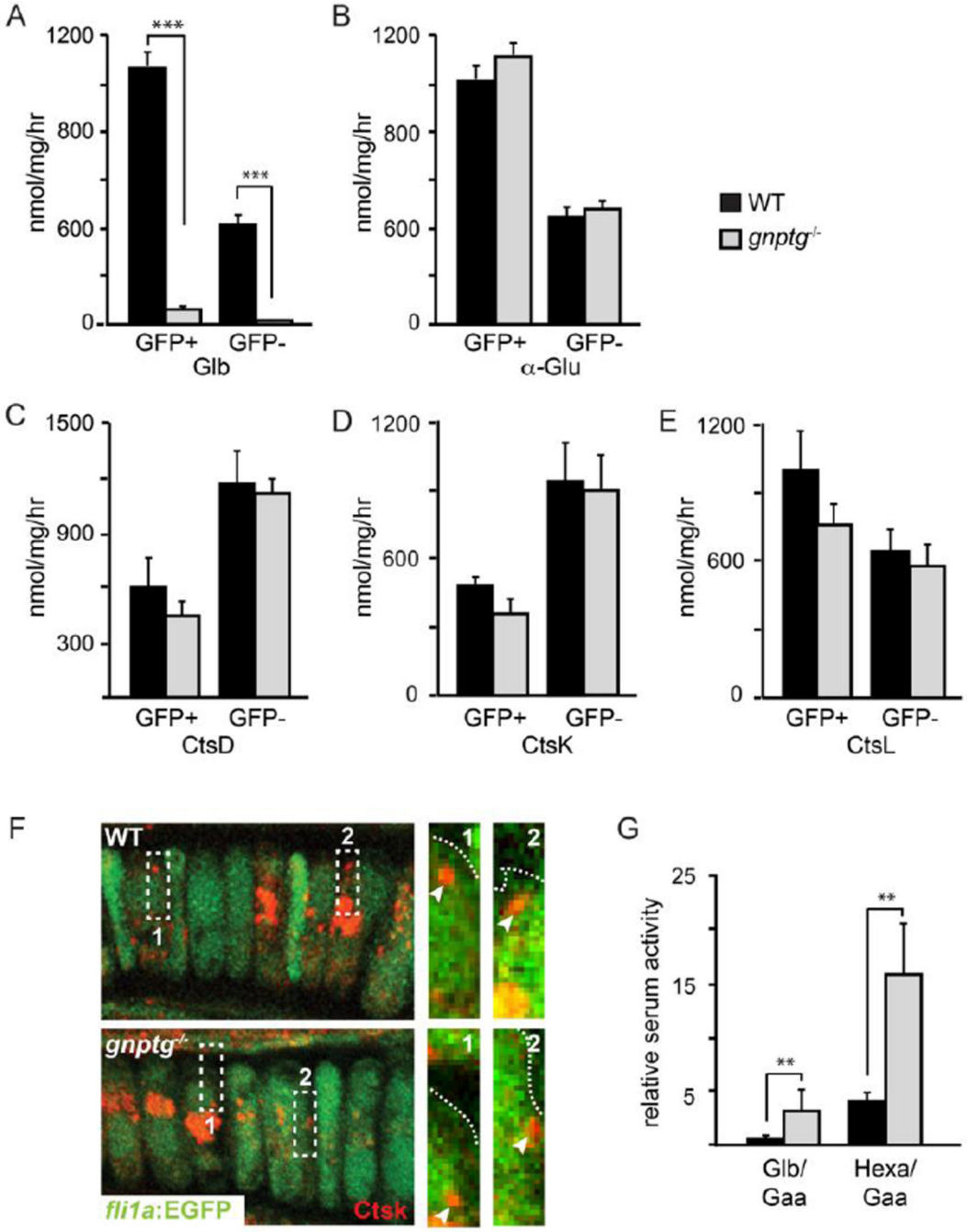

Figure 2. Several glycosidases but not cathepsin proteases are hypersecreted from *gnptg*$^{-/-}$ animals

(A,B) Glycosidase activity levels are reduced compared to WT in GFP (+) and (−) cells isolated from *gnptg*$^{-/-}$ embryos 3dpf. n=3 exper. of >500 embryos/condition. Each experiment represents a unique parental cross (i.e. biological replicate). (C-E) Cathepsin activity levels are similar in GFP (+) and (−) cells isolated from WT and *gnptg*$^{-/-}$ embryos. n=3 exper. of >500 embryos/condition. Each experiment represents a unique parental cross. (F) Confocal images of WT and *gnptg*$^{-/-}$ *fli1a*:EGFP embryos 4dpf show Ctsk protein (red) remains intracellular. This is best illustrated in higher power panels of regions of interest

(ROI1-2), where dotted lines demarcate the edge of EGFP-positive signal. Arrowheads highlight CtsK-positive signal. In 100% of the cells analyzed, Ctsk staining overlapped completely with GFP staining. Images represent maximum intensity projections of 2 compressed (0.4μM) slices. n=10 animals/condition. 20–30 cells per cartilage were analyzed. To ensure their intracellular location, red puncta close to the cell border were always looked at in high power. (G) Enzyme analyses performed on blood serum isolated from WT and *gnptg*$^{-/-}$ adult animals show higher circulating levels of β-galactosidase (Glb) and α-hexosaminidase (Hexa) in γ mutants. Enzyme activities were normalized to the activity of acid-α-glucosidase. n=5 animals/condition. ** is $p<0.01$. β-galactosidase (Glb), α-glucuronidase (Gusa), cathepsin D (Ctsd), cathepsin K (Ctsk), cathepsin L (Ctsl).

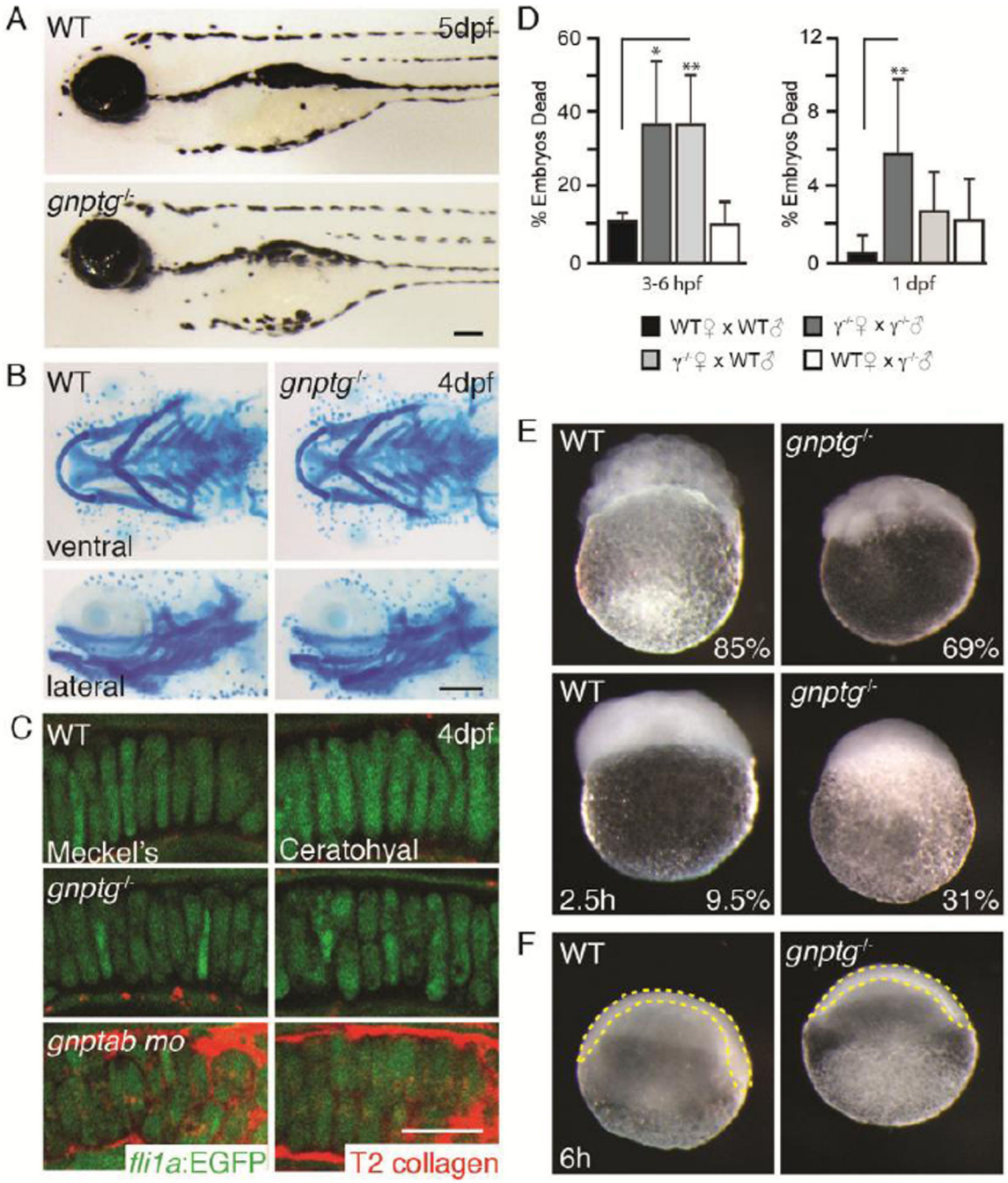

Figure 3. Although grossly normal, *gnptg*$^{-/-}$ embryos exhibit reduced fertilization and slower development than WT embryos

(A) Bright field images of embryos 5dpf show *gnptg*$^{-/-}$ embryos are grossly normal. Scale bar = 10μM. (B) Alcian blue stains of developing cartilage show no obvious defects. Percent values equal the number of embryos resembling the pictured animal. n=100 embryos over 3 experiments. Each experiment represents a unique parental cross (i.e. biological replicate). M, Meckel's and CH, ceratohyal. Scale bar =10μM. (C) Confocal images of WT, *gnptg*$^{-/-}$, and *gnptab* morphant *fli1a*:EGFP (green) embryos stained with type II collagen (red) show *gnptg*$^{-/-}$ animals lack the typical MLII phenotypes. Meckel's and ceratohyal craniofacial

cartilages shown. Percent values equal the number of embryos resembling the pictured animal. n=20 embryos, 4 cartilages per embryo assayed. Scale bar =10μM (D) Graph of embryo survival in four unique genetic crosses demonstrates significant death in both *gnptg*$^{-/-}$ (black bars) progeny and progeny of *gnptg*$^{-/-}$ mothers (white bars) during the first 3–6hpf and again 24hpf. n>300 embryos over 5 experiments. Each experiment represents a unique parental cross. (E) Bright field images of WT and *gnptg*$^{-/-}$ embryos 2.5hpf show that 31% of *gnptg*$^{-/-}$ animals remain unicellular, a phenotype only noted in 9.5% of WT embryos. Although 69% and 85% of the *gnptg*$^{-/-}$ and WT embryos proceed through cleavage, *gnptg*$^{-/-}$ embryos develop more slowly. This is evident in reduced cell number (E) and slower gastrulation (F). Consistent with standard zebrafish stages 85% of WT animals typically have 128–256 cells 2–2.5hpf, where 69% of *gnptg*$^{-/-}$ animals only have 8–16 cells. (F) 6hpf WT embryos have reached shield stage, while *gnptg*$^{-/-}$ have not. This is assessed by whether the embryo (outlined in yellow) has reached the egg midline (dashed white line).

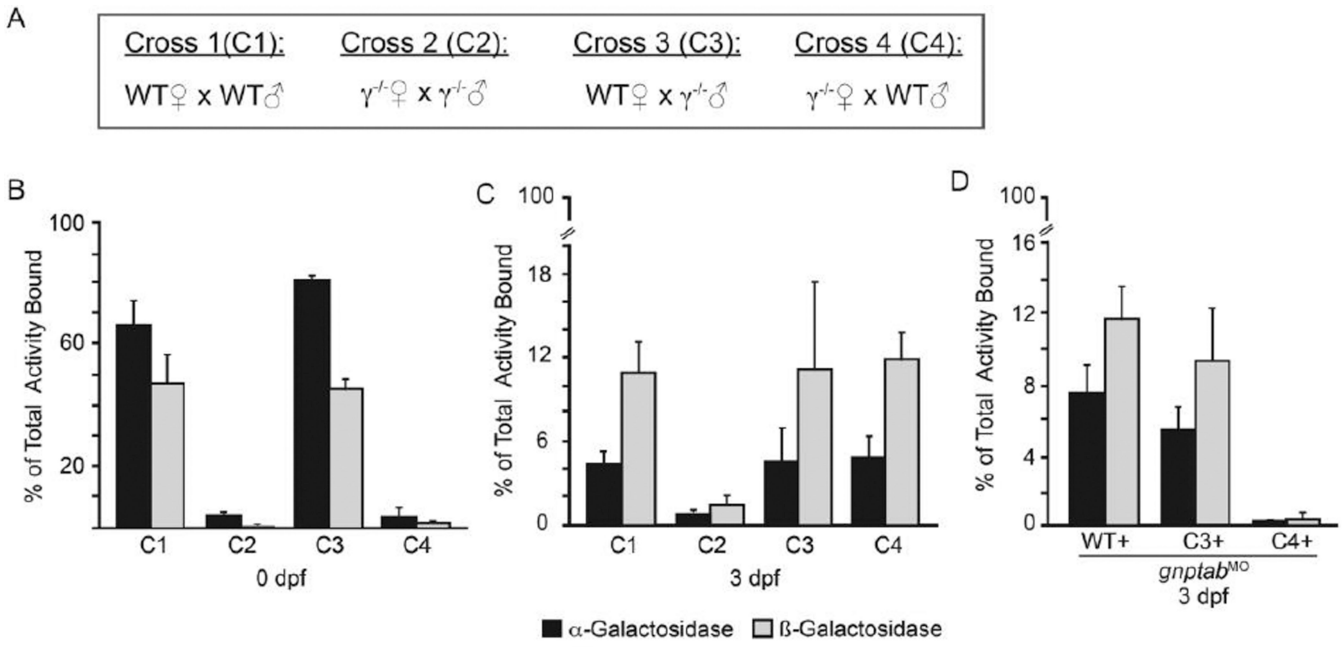

Figure 4. Deposition of M6P modified glycosidases is significantly reduced in progeny of *gnptg*$^{-/-}$ mothers

(A) Schematic outlining the four crosses performed. Man 6-P modification was assessed on α- and β-glycosidase enzymes in progeny of these crosses at (B) 0 dpf, (C) 3 dpf, and (D) in combination with *gnptab*-inhibition. n=4 experiments/condition. Each experiment represents a unique parental cross (i.e. biological replicate).

Cross 1 (C1):	Cross 2 (C2):	Cross 3 (C3):	Cross 4 (C4):
WT♀ x WT♂	$\gamma^{-/-}$♀ x $\gamma^{-/-}$♂	WT♀ x $\gamma^{-/-}$♂	$\gamma^{-/-}$♀ x WT♂

Table II. Mannose Phosphorylation of Acid Hydrolases in 0d Progeny of Crosses

Lysosomal hydrolase	% of activity bound to CI-MPR column			
	(C1) WT♀ x WT♂ (n=4)	(C2) $\gamma^{-/-}$♀ x $\gamma^{-/-}$♂ (n=4)	(C3) WT♀ x $\gamma^{-/-}$♂ (n=4)	(C4) $\gamma^{-/-}$♀ x WT♂ (n=4)
α-galactosidase	66.5 ± 7.9	4.5 ± 1.1	81.5 ± 0.8	4.2 ± 3.0
ß-galactosidase	47.2 ± 9.8	0.8 ± 0.3	46.1 ± 3.2	1.9 ± 0.9

Table III. Mannose Phosphorylation of Acid Hydrolases in 3d Progeny of Crosses

Lysosomal hydrolase	% of activity bound to CI-MPR column			
	(C1) WT♀ x WT♂ (n=4)	(C2) $\gamma^{-/-}$♀ x $\gamma^{-/-}$♂ (n=4)	(C3) WT♀ x $\gamma^{-/-}$♂ (n=4)	(C4) $\gamma^{-/-}$♀ x WT♂ (n=4)
α-galactosidase	4.5 ± 0.9	1.0 ± 0.1	4.6 ± 2.3	4.9 ± 1.5
ß-galactosidase	11.0 ± 2.2	1.5 ± 0.6	11.2 ± 6.3	11.9 ± 1.9

Table IV. Mannose Phosphorylation of Acid Hydrolases in 6d Progeny of Crosses

Lysosomal hydrolase	% of activity bound to CI-MPR column			
	(C1) WT♀ x WT♂ (n=4)	(C2) $\gamma^{-/-}$♀ x $\gamma^{-/-}$♂ (n=4)	(C3) WT♀ x $\gamma^{-/-}$♂ (n=4)	(C4) $\gamma^{-/-}$♀ x WT♂ (n=4)
α-galactosidase	8.5 ± 0.9	0.5 ± 0.1	12.8 ± 2.0	4.2 ± 1.7
ß-galactosidase	19.6 ± 4.2	1.0 ± 0.3	19.3 ± 5.7	14.4 ± 5.8

Figure 5. Table II–IV – Mannose phosphorylation of acid hydrolases in 0–6d progeny from unique genetic crosses

The progeny of 4 different genetic crosses, as indicated in boxed region, were collected at 0d (Table II), 3d (Table III), or 6d (Table IV). The level of M6P modification was assessed, as described in the Results and Materials and Methods, on α- and β-galactosidase. Genotype-specific differences in M6P levels demonstrate a role for the γ-subunit in maternal deposition of modified enzyme.

Table I

Mannose Phosphorylation of Acid Hydrolases from Zebrafish

	% of activity bound to CI-MPR column				
Lysosomal hydrolase	**WT Adult Brain (n=10)**	**γ/γ Adult Brain (n=10)**	**WT Embryos (n=7)**	**ML-II Embryos (n=7)**	**γ/γ Embryos (n=4)**
β-Galactosidase	27.8 ± 2.2	1.1 ± 2.1	17.4 ± 1.5	11.7 ± 1.9	1.43 ± 0.6
β-Glucuronidase	28.6 ± 1.4	1.2 ± 1.4	13.9 ± 3.1	7.6 ± 1.5	1.36 ± 0.5
β-Hexosaminidase	23.3 ± 3.2	4.2 ± 2.3	15.7 ± 2.3	9.4 ± 2.8	1.70 ± 0.1
Cathepsin D	24.2 ± 8.4	17.3 ± 5.1	16.4 ± 4.8	5.0 ± 2.1	12.3 ± 3.1
Cathepsin K	93.1 ± 4.0	96.4 ± 3.3	86.2 ± 5.5	17.2 ± 3.7	60.2 ± 3.6
Cathepsin L	88.8 ± 3.6	98.1 ± 6.8	82.6 ± 4.9	23.7 ± 8.8	61.0 ± 4.4
Cathepsin S	70.7 ± 15.9	64.5 ± 9.2	65.8 ± 11.2	30.1 ± 15.5	55.0 ± 8.2